How to kill bacteria

fast

and slow

A thesis submitted to attain the degree of

DOCTOR OF SCIENCES of ETH ZURICH

(Dr. sc. ETH Zurich)

presented by

MALTE MÜTTER

MSc., TU Berlin

born on December 1st, 1992

accepted on the recommendation of

Prof. Dr. Sebastian Bonhoeffer, ETH Zürich

Prof. Dr. Roland Regoes

Dr. Danie Angst

2025

Summary

Since the discovery of penicillin, antibiotics have been a cornerstone of modern medicine, saving countless lives. This achievement is now under threat, as bacteria have evolved resistance mechanisms against most available drugs. Resistance arises through the acquisition of resistance genes—either via mutations or through horizontal transfer on mobile genetic elements such as plasmids—and is selected for according to the administered drugs, their concentrations, and the pharmacodynamics that link treatment to its effect on the bacterial population.

To curb the spread of resistance, antibiotics should ideally be chosen on the basis of phenotypic information. In emergency situations, however, this is not always feasible. Therapy then relies on predefined treatment protocols rather than tailored data. Chapter 2 examines how these default protocols (treatment strategies) influence the persistence of plasmid-mediated resistance and the emergence of new double resistance. We performed large-scale automated in-vitro experiments that mimic hospital-like transmission dynamics, using two antibiotics in combination with two resistance plasmids derived from clinical isolates.

We found that administering both drugs to every patient (combination therapy) was the most effective strategy in most scenarios. Although theoretical models often predict the success of combination therapy, the clinical literature is less conclusive. This gap has several causes: some drug pairs act synergistically, whereby the combined effect exceeds the sum of single-drug effects, whereas others act antagonistically, reducing overall efficacy.

Drug interactions have so far been studied mainly at concentrations below the minimal inhibitory concentration (MIC), where growth can be tracked conveniently by optical density (OD). OD cannot measure bacterial decline, and probing the clinically relevant super-MIC range—where bacteria are actively killed—requires colony-forming-unit (CFU) assays, which are labor-intensive and unsuited to high throughput.

Chapter 3 therefore evaluates whether a luminescence-based high-throughput method, previously validated for sub-MIC conditions, can also track population dynamics across the entire concentration range. Using bacteria engineered to emit bioluminescent light, we show that this method accurately estimates net growth rates for drugs that do not induce significant filamentation.

Building on these insights, Chapter 4 explores drug interactions for six antibiotics that performed well in the preceding validation. We analysed 15 drug pairs across 144 concentration combinations each, introducing a mathematical framework to describe the pharmacodynamics of combinations. By comparing observed effects to null models of non-interaction, we classified pairs as neutral, synergistic or antagonistic, and demonstrated that interaction types can shift markedly between sub- and super-MIC conditions.

Together, these studies combine experimental and theoretical approaches to elucidate antibiotic effects on bacterial populations and resistance evolution. They deliver robust tools for quantifying population dynamics and bolster the case for combination therapy, while refining our understanding of drug–drug interactions across clinically relevant concentration ranges.

Zusammenfassung

Seit der Entdeckung des Penicillins bilden Antibiotika einen Grundpfeiler der modernen Medizin und haben unzählige Leben gerettet. Dieser Erfolg ist jedoch bedroht, da Bakterien gegen die meisten verfügbaren Wirkstoffe Resistenzmechanismen entwickelt haben. Resistenzen entstehen durch den Erwerb von Resistenzgenen – entweder über Mutationen oder durch horizontalen Gentransfer via mobile genetische Elemente wie Plasmide – und werden abhängig von verabreichten Wirkstoffen, deren Konzentrationen und den Pharmakodynamiken selektiert, die Behandlung und Wirkung miteinander verknüpfen.

Um die Ausbreitung von Resistenzen einzudämmen, sollten Antibiotika idealerweise auf Basis phänotypischer Informationen ausgewählt werden. In Notfallsituationen ist dies jedoch oft nicht möglich, sodass auf vordefinierte Behandlungsprotokolle zurückgegriffen wird. Kapitel 2 untersucht, wie diese Standardprotokolle (Behandlungsstrategien) die Persistenz plasmidvermittelter Resistenzen und das Auftreten neuer Doppelresistenzen beeinflussen. Hierfür führten wir groß angelegte, automatisierte In-vitro-Experimente durch, die krankenhausähnliche Übertragungsdynamiken simulieren; zum Einsatz kamen zwei Antibiotika in Kombination mit zwei aus klinischen Isolaten stammenden Resistenzplasmiden.

Die Gabe beider Wirkstoffe an jeden Patienten (Kombinationstherapie) erwies sich in den meisten Szenarien als wirksamste Strategie. Obwohl theoretische Modelle diesen Erfolg häufig vorhersagen, ist die klinische Datenlage weniger eindeutig. Ursachen hierfür sind unter anderem synergistische Wirkstoffpaarungen, bei denen der kombinierte Effekt größer ist als die Summe der Einzeleffekte, sowie antagonistische Paarungen, bei denen er kleiner ausfällt.

Bisher wurden Arzneimittelinteraktionen überwiegend bei Konzentrationen unterhalb der minimalen Hemmkonzentration (MIC) untersucht, da Wachstumsraten dort bequem mittels optischer Dichte (OD) erfassbar sind. OD misst jedoch keinen Bakterienrückgang. Der klinisch relevante Super-MIC-Bereich, in dem Bakterien aktiv abgetötet werden, erfordert koloniebildende Einheiten (CFU), ein arbeitsintensives und wenig durchsatzstarkes Verfahren.

Kapitel 3 prüft daher, ob eine bereits für Sub-MIC-Bedingungen validierte, lumineszenzbasierte Hochdurchsatzmethode auch über den gesamten Konzentrationsbereich einsetzbar ist. Durch gentechnisch veränderte, bioluminezente Bakterien konnten wir zeigen, dass diese Methode die Nettowachstumsrate für Wirkstoffe ohne ausgeprägte Filamentierung präzise erfasst.

Aufbauend darauf untersucht Kapitel 4 Wirkstoffinteraktionen für sechs im Vorversuch bewährte Antibiotika. Wir analysierten 15 Wirkstoffpaare mit jeweils 144 Konzentrationskombinationen und entwickelten einen mathematischen Rahmen zur Beschreibung der Pharmakodynamik von Kombinationen. Durch Vergleich der beobachteten Effekte mit Nullmodellen ohne Interaktion klassifizierten wir Paare als neutral, synergistisch oder antagonistisch und zeigten, dass sich diese Klassifikationen zwischen Sub- und Super-MIC-Bereichen deutlich ändern können.

Insgesamt verbinden diese Arbeiten experimentelle und theoretische Ansätze, um die Wirkung von Antibiotika auf bakterielle Populationen und die Resistenzentwicklung zu beleuchten. Sie liefern robuste Methoden zur Quantifizierung von Populationsdynamiken, stärken die Evidenz für Kombinationstherapien und verfeinern unser Verständnis von Arzneimittelinteraktionen über klinisch relevante Konzentrationsbereiche hinweg.

Preface

about data and stuff...

CONTENTS

1. format frontpage for papers. Do it like niko. Abstract; Authors; Contributions; and manuscript accepted/submitted/in preparation.

2. improve formatting of chapter and section titles

1 Introduction

Antibiotics have nearly eliminated premature death from bacterial infections in most parts of the developed world, to the extent that effective treatment is now often taken for granted ?. The threat to this achievement posed by antibiotic resistance was recognized early, for instance by Kirby (1944), and explicitly highlighted by Alexander Fleming in his 1945 Nobel Prize speech. Today, this threat has materialized: antimicrobial resistance (AMR) contributed to an estimated 4.71 million deaths in 2021, with 1.14 million deaths directly attributable to resistant infections Naghavi et al. (2024). The possibility of returning to a world where antibiotics are largely ineffective underscores the importance of understanding the ecological and evolutionary forces shaping AMR.

Evolution of antibiotic resistance is driven by two key processes: mutation and selection. Resistance genes arise de novo through mutations, occurring either on bacterial chromosomes or on extrachromosomal mobile genetic elements that replicate independently, such as plasmids (small circular DNA molecules) or bacteriophages (viruses targeting bacteria). Once established, these genes can spread vertically—passed from a mother cell to its offspring during cell division—or horizontally, whereby previously susceptible cells acquire resistance by taking up foreign DNA, e.g. via plasmid conjugation. While some plasmids are transmitted only vertically, others can transfer horizontally between bacterial cells via conjugation. During conjugation, plasmids initiate the formation of a pilus, a physical tunnel connecting cells, allowing DNA transfer. This mechanism facilitates gene exchange across bacterial lineages and even species boundaries ??.

Whether these emerged resistance genes can persist depends on selection. Selection is shaped by the interplay between (i) pharmacokinetics (PK), which describes how drug concentrations change over time within the host, and (ii) pharmacodynamics (PD), which describes how these concentrations influence bacterial population dynamics Regoes et al. (2004).

Each use of antibiotics imposes selective pressure on microbial populations, which can favor the

emergence or spread of resistant variants. This is consistent with the widely accepted view that antibiotic use is the main driver of resistance evolution ?. However, because infections can be life-threatening, antibiotic use is often unavoidable, creating a trade-off between effective treatment and the risk of selecting for resistant bacteria.

This raises the fundamental question of how to best use antibiotics to treat infections; with and without knowledge about the phenotypic properties of the infecting pathogen.

Treatment Strategies and Combination Therapy

In an ideal scenario, the treatment of infections is tailored to the resistance phenotype of the infecting pathogen. However, in clinical practice this is often not feasible: in emergency settings, immediate treatment is required and microbiological characterisation typically takes 24 to 72 hours ?; resistance may exist below detection thresholds, rendering diagnostics inconclusive; and in prophylactic contexts such as surgery or treatment of immunocompromised patients, antibiotics are often prescribed preemptively.

In such cases of limited information, clinicians rely on empirical treatment strategies that aim to minimize the risk of selecting for resistance. Commonly discussed approaches include combination therapy (simultaneous use of multiple antibiotics), mixing (random patient allocation to different antibiotics), and cycling (periodic rotation of antibiotics over time). Among these, combination therapy, which was first introduced in agriculture to prevent resistance in plant pathogens Kable and Jeffery (1980); Delp (1980); Skylakakis (1981) is often considered the most promising strategy in theoretical models Bonhoeffer et al. (1997); Tepekule et al. (2017); Uecker and Bonhoeffer (2021).

However, concerns persist. One major concern is that combination therapy might accelerate the selection for resistance, given the observed correlation between overall antibiotic consumption and resistance [gregory], not only regarding the targeted pathogen but also for the microbiome ?. Furthermore, combining antibiotics may impose a higher burden on patients, for example through an increased risk of toxicity Tamma et al. (2012).

In the clinical context combination therapy plays a central role in clinical protocols for rapidly evolving pathogens such as HIV, Mycobacterium tuberculosis, and Plasmodium falciparum Goldberg et al. (2012). Nonetheless, the clinical evidence remains inconclusive. A recent meta-analysis

found no consistent advantage of combination therapy in preventing resistance across bacterial infections Siedentop et al. (2024). The discrepancy between theoretical predictions and inconclusive clinical outcomes can stem both from limitations in modelling or clinical study design. On the theoretical side, models often rely on simplifying assumptions and may overlook important biological complexities, such as heterogeneity in patients, pathogens, and treatment responses. On the clinical side, most trials are not designed to detect resistance outcomes and are therefore underpowered for this purpose Siedentop et al. (2024). Additional variability arises from differences in study design, pathogens, treatment regimens, and clinical endpoints. Moreover, the choice of antibiotic combination itself can increase or decrease treatment success, further contributing to outcome variability.

To bridge the gap between theoretical models and clinical studies, Angst et al. Angst et al. (2021) developed an in vitro experimental setup that mimics the epidemiological dynamics of hospital wards under different treatment strategies. They compared the effects of combination therapy, mixing, cycling, monotherapy, and no treatment (control) on the evolution of chromosomal resistance to streptomycin and nalidixic acid in Escherichia coli. Their results showed that combination therapy was the most effective in preventing resistance evolution, while mixing and cycling were less effective, but still outperformed monotherapy in most cases.

In Chapter 2, we refined this experimental framework to study the dynamics of plasmid-mediated resistance evolution under similar clinical conditions. Specifically, we used two conjugative, compatibility-tested plasmids—originally isolated from hospital patients in a previous study Tschudin-Sutter et al. (2016) — that confer resistance to ceftazidime and tetracycline, respectively. Our results confirmed that combination therapy remains the most effective strategy even for plasmid-borne resistance, with mixing and cycling again performing better than monotherapy in most scenarios.

Population Dynamics under Combination Therapy

To better understand the potential of combination therapy, a deeper insight into drug interactions is needed. Drug interaction studies evaluate how the combined effect of two antibiotics compares to a predicted neutral effect derived from their individual actions. Two classical null models are typically used for this purpose: the Loewe additivity model Loewe and H. (1926) and the Bliss

independence model BLISS (1939). Numerous studies have investigated drug interactions below the minimum inhibitory concentration (MIC) Yeh et al. (2006), (?) providing valuable insights into sublethal interactions. However, it remains unclear whether these findings extend to the super-MIC range, where antibiotics are expected to kill bacteria. This uncertainty arises from the scarcity of studies exploring interactions above the MIC.

The reason for this is methodological: to quantify treatment effects, we estimate the exponential change in time-series population curves. Below the MIC, bacterial growth is typically quantified using optical density (OD), which allows for high-throughput measurement. However, OD does not distinguish between live and dead cells, making it unreliable for estimating net growth rates above the MIC. At super-MIC concentrations, colony-forming unit (CFU) assays remain the gold standard, but they are labor-intensive, costly, and can become unreliable at high drug levels.

To address this limitation, we evaluated in Chapter 3 whether luminescence assaysKishony and Leibler (2003), commonly used to measure growth below the MIC, remain reliable in the super-MIC range. The key assumptions for this method are: (i) light intensity is proportional to the number of living bacteria, and (ii) this proportionality remains stable over time. While (i) holds as long as bacterial density remains low enough to prevent overshadowing and the measurement setup is consistent, (ii) depends on the stability of the specific luminosity—the average light emitted per cell. To improve stability, we integrated the lux operon from the pCS-λ plasmid into the bacterial chromosome, thereby minimizing copy number effects that could alter cell-specific luminosity. We found that for antibiotics that do not induce strong filamentation, specific luminosity remains approximately constant, enabling a reliable approximation of net growth rates in the super-MIC range.

Using this method, Chapter 4 explores the pharmacodynamics of drug interactions among six antibiotics: amoxicillin, colistin, chloramphenicol, fosfomycin, polymyxinB, and tetracycline. In total, we measured interactions for 2160 drug-combination-concentration pairs. We extended the standard pharmacodynamic formalism to describe combination treatments using polar coordinates and compared the resulting curves to predictions from the Loewe additivity and Bliss independence models.

1.1 Thesis outline

BIBLIOGRAPHY

Mohsen Naghavi, Stein Emil Vollset, Kevin S. Ikuta, Lucien R. Swetschinski, Authia P. Gray, Eve E. Wool, Gisela Robles Aguilar, Tomislav Mestrovic, Georgia Smith, Chieh Han, Rebecca L. Hsu, Julian Chalek, Daniel T. Araki, Erin Chung, Catalina Raggi, Anna Gershberg Hayoon, Nicole Davis Weaver, Paulina A. Lindstedt, Amanda E. Smith, Umut Altay, Natalia V. Bhattacharjee, Konstantinos Giannakis, Frederick Fell, Barney McManigal, Nattwut Ekapirat, Jessica Andretta Mendes, Tilleye Runghien, Oraya Srimokla, Atef Abdelkader, Sherief Abd-Elsalam, Richard Gyan Aboagye, Hassan Abolhassani, Hasan Abualruz, Usman Abubakar, Hana J. Abukhadijah, Salahdein Aburuz, Ahmed Abu-Zaid, Sureerak Achalapong, Isaac Yeboah Addo, Victor Adekanmbi, Temitayo Esther Adeyeoluwa, Qorinah Estiningtyas Sakilah Adnani, Leticia Akua Adzigbli, Muhammad Sohail Afzal, Saira Afzal, Antonella Agodi, Austin J. Ahlstrom, Aqeel Ahmad, Sajjad Ahmad, Tauseef Ahmad, Ali Ahmadi, Ayman Ahmed, Haroon Ahmed, Ibrar Ahmed, Mohammed Ahmed, Saeed Ahmed, Syed Anees Ahmed, Mohammed Ahmed Akkaif, Salah Al Awaidy, Yazan Al Thaher, Samer O. Alalalmeh, Mohammad T. AlBataineh, Wafa A. Aldhaleei, Adel Ali Saeed Al-Gheethi, Nma Bida Alhaji, Abid Ali, Liaqat Ali, Syed Shujait Ali, Waad Ali, Kasim Allel, Sabah Al-Marwani, Ahmad Alrawashdeh, Awais Altaf, Alaa B. Al-Tammemi, Jaffar A. Al-Tawfiq, Karem H. Alzoubi, Walid Adnan Al-Zyoud, Ben Amos, John H. Amuasi, Robert Ancuceanu, Jason R. Andrews, Abhishek Anil, Iyadunni Adesola Anuoluwa, Saeid Anvari, Anayochukwu Edward Anyasodor, Geminn Louis Carace Apostol, Jalal Arabloo, Mosab Arafat, Aleksandr Y. Aravkin, Demelash Areda, Abdulfatai Aremu, Anton A. Artamonov, Elizabeth A. Ashley, Marvellous O. Asika, Seyyed Shamsadin Athari, Maha Moh'd Wahbi Atout, Tewachew Awoke, Sina Azadnajafabad, James Mba Azam, Shahkaar Aziz, Ahmed Y. Azzam, Mahsa Babaei, Francois Xavier Babin, Muhammad Badar, Atif Amin Baig, Milica Bajcetic, Stephen Baker, Mainak Bardhan, Hiba Jawdat Barqawi, Zarrin Basharat, Afisu Basiru, Mathieu Bastard, Saurav Basu, Nebiyou Simegnew Bayleyegn, Melaku Ashagrie

Belete, Olorunjuwon Omolaja Bello, Apostolos Beloukas, James A. Berkley, Akshaya Srikanth Bhagavathula, Sonu Bhaskar, Soumitra S. Bhuyan, Julia A. Bielicki, Nikolay Ivanovich Briko, Colin Stewart Brown, Annie J. Browne, Danilo Buonsenso, Yasser Bustanji, Cristina G. Carvalheiro, Carlos A. Castañeda-Orjuela, Muthia Cenderadewi, Joshua Chadwick, Sandip Chakraborty, Rama Mohan Chandika, Sara Chandy, Vilada Chansamouth, Vijay Kumar Chattu, Anis Ahmad Chaudhary, Patrick R. Ching, Hitesh Chopra, Fazle Rabbi Chowdhury, Dinh Toi Chu, Muhammad Chutiyami, Natalia Cruz-Martins, Alanna Gomes da Silva, Omid Dadras, Xiaochen Dai, Samuel D. Darcho, Saswati Das, Fernando Pio De La Hoz, Denise Myriam Dekker, Kuldeep Dhama, Daniel Diaz, Benjamin Felix Rothschild Dickson, Serge Ghislain Djorie, Milad Dodangeh, Sushil Dohare, Klara Georgieva Dokova, Ojas Prakashbhai Doshi, Robert Kokou Dowou, Haneil Larson Dsouza, Susanna J. Dunachie, Arkadiusz Marian Dziedzic, Tim Eckmanns, Abdelaziz Ed-Dra, Aziz Eftekharimehrabad, Temitope Cyrus Ekundayo, Iman El Sayed, Muhammed Elhadi, Waseem El-Huneidi, Christelle Elias, Sally J. Ellis, Randa Elsheikh, Ibrahim Elsohaby, Chadi Eltaha, Babak Eshrati, Majid Eslami, David William Eyre, Adewale Oluwaseun Fadaka, Adeniyi Francis Fagbamigbe, Ayesha Fahim, Aliasghar Fakhri-Demeshghieh, Folorunso Oludayo Fasina, Modupe Margaret Fasina, Ali Fatehizadeh, Nicholas A. Feasey, Alireza Feizkhah, Ginenus Fekadu, Florian Fischer, Ida Fitriana, Karen M. Forrest, Celia Fortuna Rodrigues, John E. Fuller, Muktar A. Gadanya, Márió Gajdács, Aravind P. Gandhi, Esteban E. Garcia-Gallo, Denise O. Garrett, Rupesh K. Gautam, Miglas Welay Gebregergis, Mesfin Gebrehiwot, Teferi Gebru Gebremeskel, Christine Geffers, Leonidas Georgalis, Ramy Mohamed Ghazy, Mahaveer Golechha, Davide Golinelli, Melita Gordon, Snigdha Gulati, Rajat Das Gupta, Sapna Gupta, Vijai Kumar Gupta, Awoke Derbie Habteyohannes, Sebastian Haller, Harapan Harapan, Michelle L. Harrison, Ahmed I. Hasaballah, Ikramul Hasan, Rumina Syeda Hasan, Hamidreza Hasani, Andrea Haekyung Haselbeck, Md Saquib Hasnain, Ikrama Ibrahim Hassan, Shoaib Hassan, Mahgol Sadat Hassan Zadeh Tabatabaei, Khezar Hayat, Jiawei He, Omar E. Hegazi, Mohammad Heidari, Kamal Hezam, Ramesh Holla, Marianne Holm, Heidi Hopkins, Md Mahbub Hossain, Mehdi Hosseinzadeh, Sorin Hostiuc, Nawfal R. Hussein, Le Duc Huy, Elsa D. Ibáñez-Prada, Adalia Ikiroma, Irena M. Ilic, Sheikh Mohammed Shariful Islam, Faisal Ismail, Nahlah Elkudssiah Ismail, Chidozie Declan Iwu, Chinwe Juliana Iwu-Jaja, Abdollah Jafarzadeh, Fatoumatta Jaiteh, Reza Jalilzadeh Yengejeh, Roland Dominic G.

Jamora, Javad Javidnia, Talha Jawaid, Adam W.J. Jenney, Hyon Jin Jeon, Mohammad Jokar, Nabi Jomehzadeh, Tamas Joo, Nitin Joseph, Zul Kamal, Kehinde Kazeem Kanmodi, Rami S. Kantar, James Apollo Kapisi, Ibraheem M. Karaye, Yousef Saleh Khader, Himanshu Khajuria, Nauman Khalid, Faham Khamesipour, Ajmal Khan, Mohammad Jobair Khan, Muhammad Tariq Khan, Vishnu Khanal, Feriha Fatima Khidri, Jagdish Khubchandani, Suwimon Khusuwan, Min Seo Kim, Adnan Kisa, Vladimir Andreevich Korshunov, Fiorella Krapp, Ralf Krumkamp, Mohammed Kuddus, Mukhtar Kulimbet, Dewesh Kumar, Emmanuelle A.P. Kumaran, Ambily Kuttikkattu, Hmwe Hmwe Kyu, Iván Landires, Basira Kankia Lawal, Thao Thi Thu Le, Ingeborg Maria Lederer, Munjae Lee, Seung Won Lee, Alain Lepape, Temesgen Leka Lerango, Virendra S. Ligade, Cherry Lim, Stephen S. Lim, Liknaw Workie Limenh, Chaojie Liu, Xiaofeng Liu, Xuefeng Liu, Michael J. Loftus, Hawraz Ibrahim M. Amin, Kelsey Lynn Maass, Sandeep B. Maharaj, Mansour Adam Mahmoud, Panagiota Maikanti-Charalampous, Omar M. Makram, Kashish Malhotra, Ahmad Azam Malik, Georgia D. Mandilara, Florian Marks, Bernardo Alfonso Martinez-Guerra, Miquel Martorell, Hossein Masoumi-Asl, Alexander G. Mathioudakis, Juergen May, Theresa A. McHugh, James Meiring, Hadush Negash Meles, Addisu Melese, Endalkachew Belayneh Melese, Giuseppe Minervini, Nouh Saad Mohamed, Shafiu Mohammed, Syam Mohan, Ali H. Mokdad, Lorenzo Monasta, Amir Ali Moodi Ghalibaf, Catrin E. Moore, Yousef Moradi, Elias Mossialos, Vincent Mougin, George Duke Mukoro, Francesk Mulita, Berit Muller-Pebody, Efren Murillo-Zamora, Sani Musa, Patrick Musicha, Lillian A. Musila, Saravanan Muthupandian, Ahamarshan Jayaraman Nagarajan, Pirouz Naghavi, Firzan Nainu, Tapas Sadasivan Nair, Hastyar Hama Rashid Najmuldeen, Zuhair S. Natto, Javaid Nauman, Biswa Prakash Nayak, G. Takop Nchanji, Pacifique Ndishimye, Ionut Negoi, Ruxandra Irina Negoi, Seyed Aria Nejadghaderi, Quynh Anh P. Nguyen, Efaq Ali Noman, Davis C. Nwakanma, Seamus O'Brien, Theresa J. Ochoa, Ismail A. Odetokun, Oluwaseun Adeolu Ogundijo, Tolulope R. Ojo-Akosile, Sylvester Reuben Okeke, Osaretin Christabel Okonji, Andrew T. Olagunju, Antonio Olivas-Martinez, Abdulhakeem Abayomi Olorukooba, Peter Olwoch, Kenneth Ikenna Onyedibe, Edgar Ortiz-Brizuela, Olayinka Osuolale, Pradthana Ounchanum, Oyetunde T. Oyeyemi, P. A.Mahesh Padukudru, Jose L. Paredes, Romil R. Parikh, Jay Patel, Shankargouda Patil, Shrikant Pawar, Anton Y. Peleg, Prince Peprah, João Perdigão, Carlo Perrone, Ionela Roxana Petcu, Koukeo Phommasone, Zahra Zahid Piracha, Dimitri Poddighe, Andrew J. Pollard, Ramesh

Poluru, Alfredo Ponce-De-Leon, Jagadeesh Puvvula, Farah Naz Qamar, Nameer Hashim Qasim, Clotaire Donatien Rafai, Pankaja Raghav, Leila Rahbarnia, Fakher Rahim, Vafa Rahimi-Movaghar, Mosiur Rahman, Muhammad Aziz Rahman, Hazem Ramadan, Shakthi Kumaran Ramasamy, Pushkal Sinduvadi Ramesh, Pramod W. Ramteke, Rishabh Kumar Rana, Usha Rani, Mohammad Mahdi Rashidi, Devarajan Rathish, Sayaphet Rattanavong, Salman Rawaf, Elrashdy Moustafa Mohamed Redwan, Luis Felipe Reyes, Tamalee Roberts, Julie V. Robotham, Victor Daniel Rosenthal, Allen Guy Ross, Nitai Roy, Kristina E. Rudd, Cameron John Sabet, Basema Ahmad Saddik, Mohammad Reza Saeb, Umar Saeed, Sahar Saeedi Moghaddam, Weeravoot Saengchan, Mohsen Safaei, Amene Saghazadeh, Narjes Saheb Sharif-Askari, Amirhossein Sahebkar, Soumya Swaroop Sahoo, Maitreyi Sahu, Morteza Saki, Nasir Salam, Zikria Saleem, Mohamed A. Saleh, Yoseph Leonardo Samodra, Abdallah M. Samy, Aswini Saravanan, Maheswar Satpathy, Austin E. Schumacher, Mansour Sedighi, Samroeng Seekaew, Mahan Shafie, Pritik A. Shah, Samiah Shahid, Moyad Jamal Shahwan, Sadia Shakoor, Noga Shalev, Muhammad Aaqib Shamim, Mohammad Ali Shamshirgaran, Anas Shamsi, Amin Sharifan, Rajesh P. Shastry, Mahabalesh Shetty, Aminu Shittu, Sunil Shrestha, Emmanuel Edwar Siddig, Theologia Sideroglou, Jose Sifuentes-Osornio, Luís Manuel Lopes Rodrigues Silva, Eric A.F. Simões, Andrew J.H. Simpson, Amit Singh, Surjit Singh, Robert Sinto, Sameh S.M. Soliman, Soroush Soraneh, Nicole Stoesser, Temenuga Zhekova Stoeva, Chandan Kumar Swain, Lukasz Szarpak, T. Y. Sree Sudha, Shima Tabatabai, Celine Tabche, Zanan Mohammed Ameen Taha, Ker Kan Tan, Nidanuch Tasak, Nathan Y. Tat, Areerat Thaiprakong, Pugazhenthan Thangaraju, Caroline Chepngeno Tigoi, Krishna Tiwari, Marcos Roberto Tovani-Palone, Thang Huu Tran, Munkhtuya Tumurkhuu, Paul Turner, Aniefiok John Udoakang, Arit Udoh, Noor Ullah, Saeed Ullah, Asokan Govindaraj Vaithinathan, Mario Valenti, Theo Vos, Huong T.L. Vu, Yasir Waheed, Ann Sarah Walker, Judd L. Walson, Tri Wangrangsimakul, Kosala Gayan Weerakoon, Heiman F.L. Wertheim, Phoebe C.M. Williams, Asrat Arja Wolde, Teresa M. Wozniak, Felicia Wu, Zenghong Wu, Mukesh Kumar Kumar Yadav, Sajad Yaghoubi, Zwanden Sule Yahaya, Amir Yarahmadi, Saber Yezli, Yazachew Engida Yismaw, Dong Keon Yon, Chun Wei Yuan, Hadiza Yusuf, Fathiah Zakham, Giulia Zamagni, Haijun Zhang, Zhi Jiang Zhang, Magdalena Zielińska, Alimuddin Zumla, Sa'ed H.H. Zyoud, Samer H. Zyoud, Simon I. Hay, Andy Stergachis, Benn Sartorius, Ben S. Cooper, Christiane Dolecek, and Christopher J.L. Murray. Global burden

of bacterial antimicrobial resistance 1990–2021: a systematic analysis with forecasts to 2050. Lancet, 404(10459):1199–1226, sep 2024. ISSN 1474547X. doi: 10.1016/S0140-6736(24)01867-1/ATTACHMENT/4F9FA746-A486-4BC0-BF71-075D4D1D6D56/MMC3.PDF. URL https://www.thelancet.com/action/showFullText?pii=S0140673624018671https://www.thelancet.com/action/showAbstract?pii=S0140673624018671https://www.thelancet.com/journals/lancet/article/PIIS0140-6736(24)01867-1/abstract.

Roland R. Regoes, Camilla Wiuff, Renata M. Zappala, Kim N. Garner, Fernando Baquero, and Bruce R. Levin. Pharmacodynamic functions: A multiparameter approach to the design of antibiotic treatment regimens. Antimicrob. Agents Chemother., 48(10):3670–3676, 2004. ISSN 00664804. doi: 10.1128/AAC.48.10.3670-3676.2004.

P. F. Kable and H. Jeffery. Selection for Tolerance in Organisms Exposed to Sprays of Biocide Mixtures: A Theoretical Model. Phytopathology, 70(1):8–12, 1980. ISSN 0031-949X. doi: 10.1094/phyto-70-8.

Charles J. Delp. Coping with resistance to plant disease. Plant Dis., 64:652–657, 1980. doi: 10.1094/PD-64-652.

George Skylakakis. Effects of Alternating and Mixing Pesticides on the Buildup of Fungal Resistance. Phytopathology, 71(11):1119 – 1121, 1981. ISSN 0031-949X. doi: 10.1094/phyto-71-1119.

Sebastian Bonhoeffer, Marc Lipsitch, and Bruce R. Levin. Evaluating treatment protocols to prevent antibiotic resistance. Proc. Natl. Acad. Sci. U. S. A., 94(22):12106–12111, 1997. ISSN 00278424. doi: 10.1073/pnas.94.22.12106.

Burcu Tepekule, Hildegard Uecker, Isabel Derungs, Antoine Frenoy, and Sebastian Bonhoeffer. Modeling antibiotic treatment in hospitals: A systematic approach shows benefits of combination therapy over cycling, mixing, and mono-drug therapies. PLoS Comput. Biol., 13(9):1–22, 2017. ISSN 15537358. doi: 10.1371/journal.pcbi.1005745.

Hildegard Uecker and Sebastian Bonhoeffer. Antibiotic treatment protocols revisited: The challenges of a conclusive assessment by mathematical modelling. J. R. Soc. Interface, 18(181), 2021. ISSN 17425662. doi: 10.1098/rsif.2021.0308.

Pranita D. Tamma, Sara E. Cosgrove, and Lisa L. Maragakis. Combination therapy for treatment of infections with gram-negative bacteria. Clin. Microbiol. Rev., 25(3):450–470, 2012. ISSN 08938512. doi: 10.1128/CMR.05041-11.

Daniel E. Goldberg, Robert F. Siliciano, and William R. Jacobs. Outwitting evolution: Fighting drug-resistant TB, Malaria, and HIV. Cell, 148(6):1271–1283, 2012. ISSN 10974172. doi: 10.1016/j.cell.2012.02.021. URL http://dx.doi.org/10.1016/j.cell.2012.02.021.

Berit Siedentop, Viacheslav N Kachalov, Christopher Witzany, Matthias Egger, D Roger, and Sebastian Bonhoeffer. The effect of combining antibiotics on resistance : A systematic review and meta-analysis. Elife, 13:1–25, 2024. doi: 10.7554/eLife.93740.1.

Daniel C. Angst, Burcu Tepekule, Lei Sun, Balázs Bogos, and Sebastian Bonhoeffer. Comparing treatment strategies to reduce antibiotic resistance in an in vitro epidemiological setting. Proc. Natl. Acad. Sci. U. S. A., 118(13):1–7, 2021. ISSN 10916490. doi: 10.1073/PNAS.2023467118.

Sarah Tschudin-Sutter, Reno Frei, Friedbert Schwahn, Milanka Tomic, Martin Conzelmann, Anne Stranden, and Andreas F. Widmer. Prospective validation of cessation of contact precautions for extended-spectrum β-lactamase-producing Escherichia coli1. Emerg. Infect. Dis., 22(6):1094–1097, 2016. ISSN 10806059. doi: 10.3201/eid2206.150554.

S. Loewe and Muischnek H. Über Kombinationswirkungen. 1926.

C. I. BLISS. the Toxicity of Poisons Applied Jointly. Ann. Appl. Biol., 26(3):585–615, 1939. ISSN 17447348. doi: 10.1111/j.1744-7348.1939.tb06990.x.

Pamela Yeh, Ariane I. Tschumi, and Roy Kishony. Functional classification of drugs by properties of their pairwise interactions. Nat. Genet., 38(4):489–494, 2006. ISSN 10614036. doi: 10.1038/ng1755.

Roy Kishony and Stanislas Leibler. Environmental stresses can alleviate the average deleterious effect of mutations. J. Biol., 2(2):1–10, 2003. ISSN 14785854. doi: 10.1186/1475-4924-2-14.

2 The Impact of Treatment Strategies on the Epidemiological Dynamics of Plasmid-Conferred Antibiotic Resistance

2.1 abstract

The issue of antibiotic resistance is a critical concern for public health, prompting numerous investigations into the impact of treatment strategies on preventing or slowing down the emergence of resistance. While existing studies have predominantly focused on chromosomal resistance mutations, the consequences of often clinically more relevant plasmid-conferred resistance remain insufficiently explored.

To address this gap, we conducted three extensive in vitro experiments utilising a liquid-handling platform. These experiments evaluated the efficacy of five distinct treatment strategies using two antibiotics (tetracycline and ceftazidime) along with two horizontally transmissible clinical resistance plasmids conferring the respective resistances.

Among the experimentally investigated treatment strategies, combination therapy proved to be the most effective in preventing the emergence of double resistance while minimising the number of infections.

To verify the reliability of these findings, we constructed a computational model of our experiments that we parameterised using the experimental data. We employed this model to augment the experimental data by conducting an in silico parameter sensitivity analysis. The sensitivity analysis corroborated our experimental results, demonstrating that combination therapy consistently outperformed other treatment strategies across a range of parameter values.

2.2 Introduction

In light of the growing threat of antimicrobial resistance (AMR) to human health, various multidrug strategies are being considered to improve the sustainability of antibiotic use. These approaches include combination therapy (simultaneous use of multiple antibiotics), mixing therapy

(randomly assigning patients to receive different antibiotics), and cycling therapy (alternating between multiple antibiotics over time).

Combination, originally proposed alongside cycling therapy to prevent biocide resistance in plant pathogens Kable and Jeffery (1980); Delp (1980); Skylakakis (1981), was later adopted in human medicine. Combination therapy proved its effectiveness in preventing resistance evolution in highly adaptable pathogens such as HIV, Mycobacterium tuberculosis, and Plasmodium falciparum Goldberg et al. (2012). However, a recent meta-analysis investigating the effect of combination therapy on resistance across various bacterial infections and antibiotic combinations found no evidence for a difference in the risk of resistance acquisition Siedentop et al. (2024). Also, a comprehensive cluster-randomised crossover study comparing mixing and cycling by van Duijn et al. van Duijn et al. (2018), spanning nearly two years across eight ICUs, found no significant differences in outcomes.

A review of the available model literature by Uecker et al. Uecker and Bonhoeffer (2021) reveals the complexity and context-dependent efficacy of treatment strategies such as combination, cycling or mixing strategies. Yet, theoretical models often identify combination therapy as the best strategy to prevent new resistance Bonhoeffer et al. (1997); Tepekule et al. (2017). It remains unclear whether the inconclusive results regarding the effectiveness of multidrug treatment strategies in the literature are due to the theoretical models failing to account for key processes, or if clinical studies lack statistical power, as suggested by Siedentop et al. Siedentop et al. (2024). This lack of power may be caused by patient and bacterial strain heterogeneity, stochasticity in infection dynamics, and other unknown factors that make it difficult to isolate single effects.

We recently started experiments to make a foray into the large gap between theoretical models and clinical trials. In an in vitro experiment mimicking the epidemiological scenario of transmission in a hospital ward, Angst et al. Angst et al. (2021) investigated the effect of cycling, mixing, and combination therapy on resistance evolution and showed that for chromosomal resistance mutations combination therapy outperformed the other strategies. One potential reason why combination therapy succeeded in that study and tends to be superior in mathematical models is that it increases the genetic barrier to resistance by requiring the acquisition of multiple mutations in the same background.

Here, we explore the effect of horizontal gene transfer (HGT) on resistance evolution under

treatment by conducting three large-scale in vitro experiments. The experiments mimic epidemiological transmission dynamics of symptomatic infections by a focal strain in an intensive care unit (ICU) and include patient discharge and admission, infection between patients, and treatment. We use two antibiotics, ceftazidime (A) and tetracycline (B), along with two clinical resistance plasmids Huisman et al. (2022) we call p_A and p_B, conferring resistance to the corresponding antibiotics. The plasmids are compatible, can conjugate, and were isolated from clinical samples collected and characterised in a study at University Hospital Basel Tschudin-Sutter et al. (2016). We model patients as wells in a 384-well microtiter plate filled with LB medium. These "patients" can be infected with a mixture of bacteria, which may carry up to two resistance plasmids. Depending on the presence of bacteria and resistance, we assign each "patient" a resistance profile: uninfected (U), sensitive infected (S), single-resistant (A_r, B_r, or (A_r&B_r)), or double-resistant (AB_r).

In each experiment, we model six hospital wards to assess the ability of five treatment strategies (mixing, cycling, combination therapy with two antibiotics and two monotherapies with each antibiotic alone) and one control (no antibiotics) to contain the spread of plasmid-borne resistance and prevent the emergence of double resistance. All patients in each ward are treated daily according to the assigned strategy. A schematic of the experimental setup is shown in Figure S1. Each of the three experiments addresses a different scenario (Table 2.1), varying in patient turnover probability (admission/discharge), infection probability, and the distribution of resistance profiles for incoming patients (sampling proportions). The prevention scenario addresses a situation with low levels of pre-existing single and no double resistance brought into the hospital ward from the community. The containment scenario focuses on the ability of treatment strategies to contain pre-existing double resistance and in the maximum-emergence scenario, we maximised the opportunities for emerging double resistance through HGT by admitting single-resistant patients only.

Alongside our experiments, we created a computational model that mimics the experiment and is parameterised but not fitted using the experimental data. We used the model to assess the robustness of our findings to the randomisation of the experimental decisions and conducted an in silico sensitivity analysis to augment the experimental data.

2.3 Results

In each of our three experiments, we simulated the transition dynamics across six hospital wards on six 384-well plates. Each 384-well plate simulates four replicate hospital wards, with each replicate comprising 96 wells representing 94 patients and two negative controls. We replace each assay plate daily to renew the treatment and medium (Figure S1). Based on the turnover probability τ, we randomly decide if a patient stays. If this is the case, we inoculate the well on the new plate from the same well on the old plate. Else we replace this patient with a new incoming patient by inoculating the well on the new plate from a strain plate containing all resistance profiles. The resistance profile of the incoming patient is randomly selected based on predefined probabilities (sampling proportions c_ϕ). Based on the infection probability β, we randomly decide if a patient will infect another randomly chosen patient. These infections are then simulated in vitro by passing a drop to the infected well on the new plate. All inoculations are carried out using the same pintool.

Multidrug strategies keep the overall number of infections lowest and best suppress single resistance. The prevention scenario is characterised by a moderate proportion of single-resistant admissions to the hospital ward, the absence of pre-existing double resistance, and a moderately spreading infection dynamic ($R_0 = 1.5$, Equation S1, SI Methods). In this scenario, there are no differences between combination, mixing, and cycling on the frequency of uninfected, single-resistant-infected and double-resistant-infected wells (Fig. 2.1A, time series in Figure S2). However, all multidrug strategies are significantly better at suppressing single resistance and increasing the number of cleared wells than the single-drug strategies and the control without treatment (Fig. 2.1A). In all scenarios, combination therapy was one of the most successful treatment strategies in minimising single-resistant and overall infections. At the same time, we

Table 2.1 Parameter sets and R_0 used in the three experiments: c_ϕ is the proportion of admitted patients with resistance profile ϕ, τ denotes the probability that a patient is replaced with a new patient sampled from the community and β denotes the infection probability.

scenario	c_S	c_{Ar}	c_{Br}	c_{ABr}	c_U	τ	β	R_0
prevention	0.75	0.05	0.05	0	0.15	0.20	0.30	1.5
containment	0.58	0.11	0.11	0.05	0.15	0.20	0.35	1.75
maximum-emergence	0	0.50	0.50	0	0	0.50	0.25	0.5

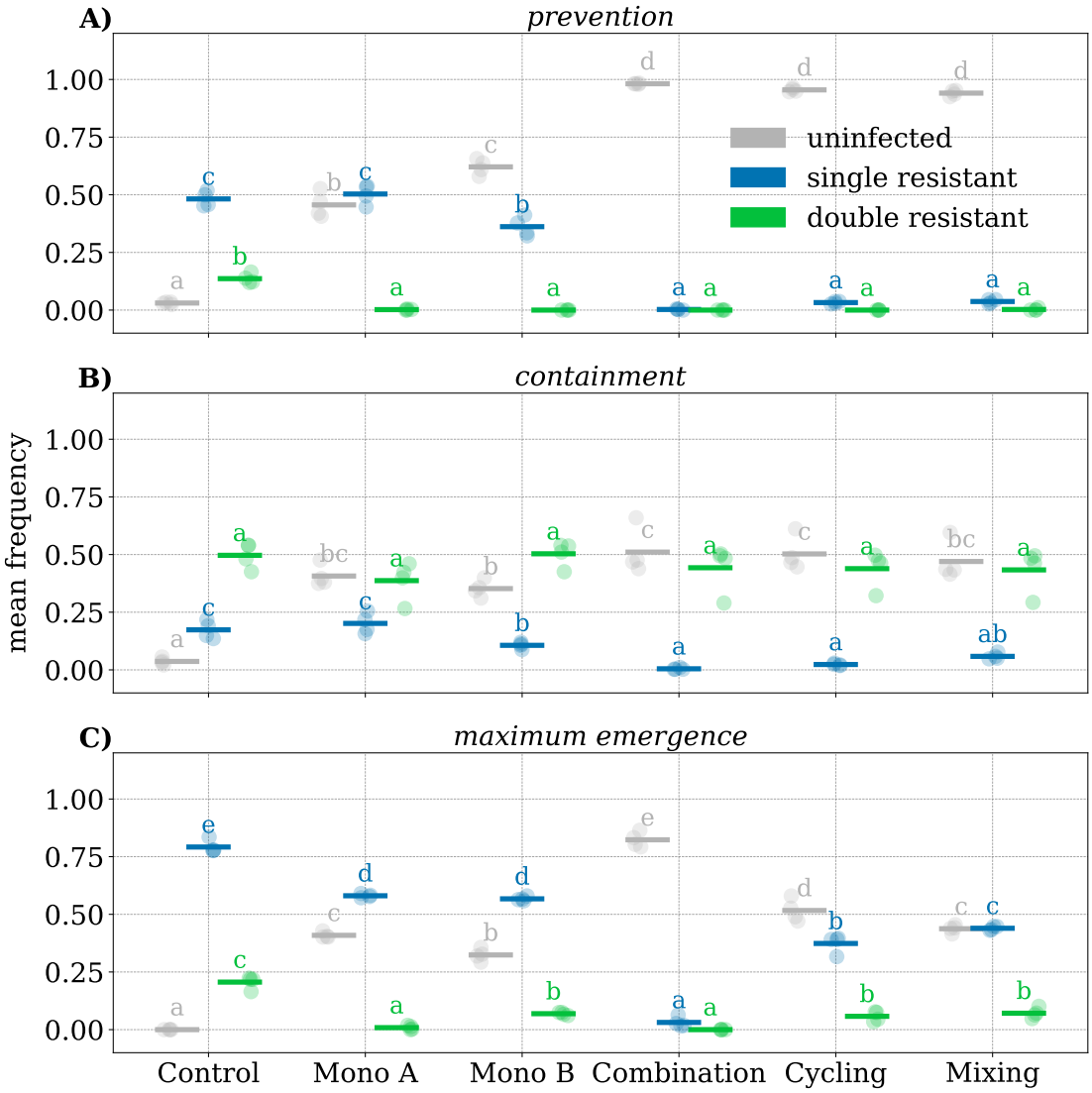

Fig. 2.1 Panels A–C show the mean frequency of uninfected (grey), single-resistant infected (blue), and double-resistant infected wells (green) during the last four transfers of the three scenarios. Circles represent replicates (n = 4), and bars represent means. Within resistance categories, bars not sharing a letter are significantly different (pairwise Tukey post hoc test, $p < 0.05$; ANOVA tables and all p-values can be found in Table S34 – S50).

observed most single and double resistance in the untreated control. All strategies (but not the control) were able to clear sensitive infections effectively with clearance probabilities of 97% for drug A, 73% for drug B, and 86% for AB (Table S8).

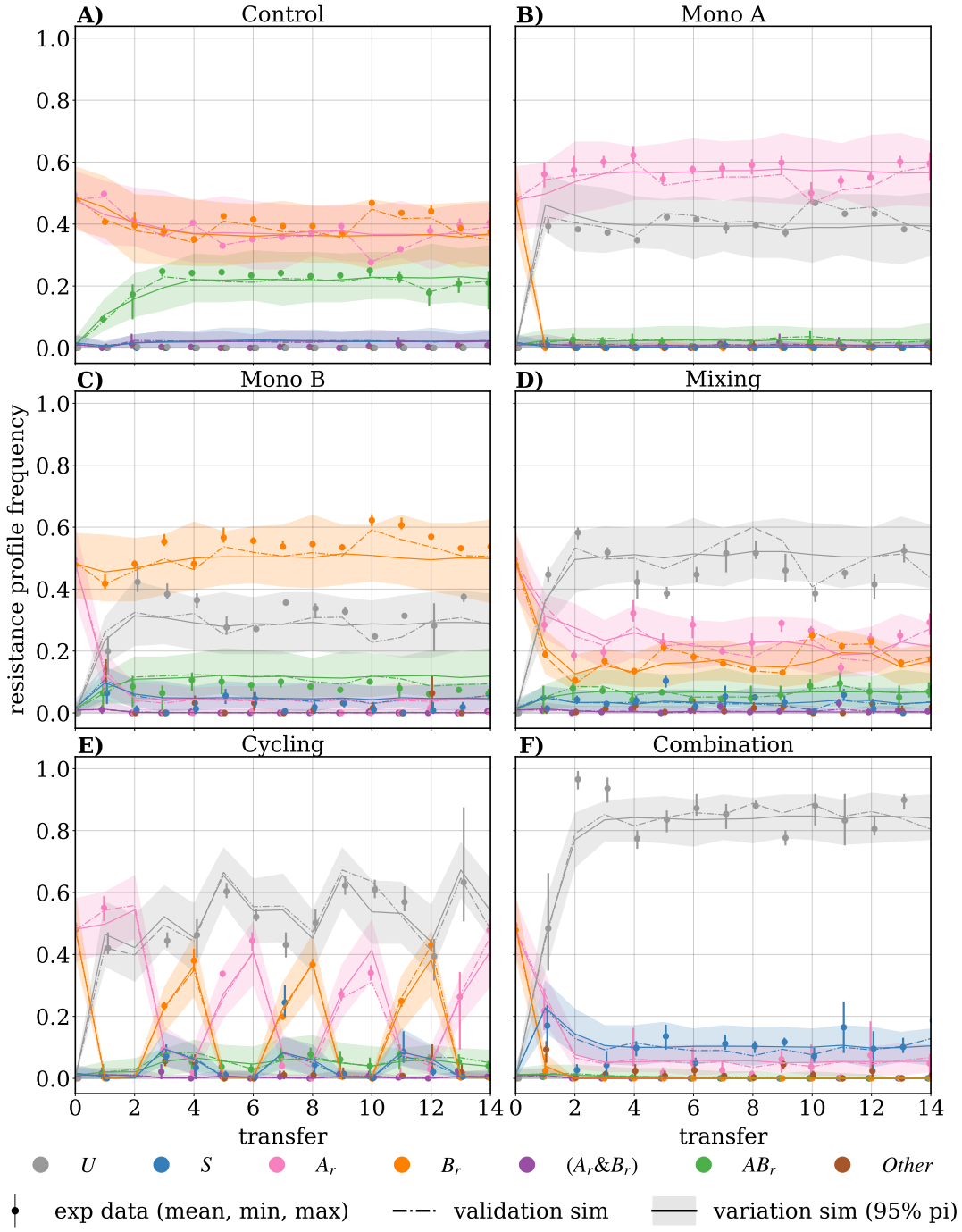

Fig. 2.2 Frequencies of resistance profiles over time during the maximum-emergence scenario. Panels (A–F) show the six tested strategies. Dots and bars show the mean and min/max interval of the four replicates. The dash-dotted line shows the mean value of 100 stochastic simulations based on the instruction set used in the in vitro experiment (validation simulation). The solid line shows the mean value of 100 simulations with randomly created instruction sets based on the parameter set used in the experiment (variation simulations). The shaded error band indicates the 95-percentile interval between the variation simulations.

All treatment strategies fail to contain pre-existing double resistance. The containment scenario explores a situation in which patients infected with double-resistant bacteria are continuously admitted to the hospital. No strategy was able to contain the spread of double resistance, resulting in increased frequencies of double resistance ($> 40\%$) in all treatment arms at the conclusion of the experiment (Fig. 2.1B).

Treatment strategies affect the emergence of double resistance. In our experiments, double resistance primarily emerges in wells inoculated with both single-resistance plasmids via HGT, as the evolution of de novo resistance (e.g. by point mutations) to high drug concentrations ($> 50\times$MIC) is unlikely. As the inoculum volumes for turnover, infection, and passage are identical in our experiments, we do not distinguish between wells containing A-resistance (A_r) infecting wells containing B-resistance (B_r) or vice versa and simply refer to these events as superinfections.

During the prevention and containment scenario, we could not identify differences in the strategies' abilities to suppress the emergence of double resistance. We attribute this to a lack of statistical power because we observed only a few instances of double resistance emerging, mostly in the untreated control. To address this, we selected parameters for the maximum-emergence scenario designed to maximise superinfection opportunities between wells carrying complementary resistance. To this end, all admitted patients carried bacteria with only one of the two resistance plasmids (at equal proportions). In addition, we set the probability of admission and discharge to $\tau = 0.5$ and the infection probability to $\beta = 0.25$, resulting in a basic reproduction number $R_0 = 0.5$ (Equation S1). An $R_0 < 1$ makes double resistance more likely to be replaced by newly admitted patients than to spread, thus maintaining a high potential for emergence. We implement this scenario to explore emergence under a magnifying glass, being aware that it does not reflect a likely clinical situation. In this scenario, combination therapy and monotherapy with drug A lead to the lowest frequency of double resistance during the last four transfers (Fig. 2.1C, Fig. 2.2).

For the maximum-emergence scenario, we observed that combination therapy, cycling, and monotherapy with drug A were most effective in preventing newly emerging double resistance. Combination was the only strategy in which we did not observe a single case of emerging double resistance after the first transfer (Fig. 2.3A). Furthermore, combination therapy is the most successful treatment strategy in minimising the number of both single-resistant and overall infec-

tions, while the control leads to the highest number of double- and single-resistant, and overall infections.

Combination therapy suppresses the emergence of double resistance by preventing superinfections. Treatment strategies can impact the emergence of double resistance by suppressing superinfections. The number of superinfections $n_{\mathscr{S}}$ is dependent on the abundance of the single resistance carrying wells A_r and B_r. Hence, we expect the highest number of superinfections and most opportunities for emerging double resistance when both single resistances are unaffected by the treatment and the fewest if the treatment successfully suppresses both single resistances. Our measurements confirmed these expectations during the maximum-emergence scenario. Here $n_{\mathscr{S}}$ is highest in the control group (no treatment) and lowest under combination therapy (Fig. 2.3B).

Treatment strategies influence the emergence of double resistance within superinfected wells. We observed the highest average frequency of superinfections developing double resistance ($\frac{n_{\mathscr{E}}}{n_{\mathscr{S}}}$) in antibiotic-free medium and in medium treated with antibiotic B (tetracycline). In contrast, superinfections resulting in double resistance rarely occur in medium treated with antibiotic A (ceftazidime) or both drugs (Fig. 2.3C). We think the impact of treatment on cell densities within superinfected wells (both in infected and infecting wells) can best explain these findings.

Firstly, applying a drug affects the in-well population dynamics of superinfected wells. Reducing the cell density for one or both single-resistant strains within a superinfected well reduces the probability of bacteria with complementary resistance to encounter and conjugate (see SI Results). As drug A (bactericidal) decreases the cell density faster than drug B (bacteriostatic), more conjugation opportunities occur in wells treated with drug B.

Secondly, the treatment strategies influence the number of transferred single-resistant bacteria that inoculate superinfections by curbing the bacterial density within the infecting wells (see SI Results).

Due to the differences in the abilities of drugs A and B to prevent conjugation, there are times (cycles) and places (beds) during cycling and mixing where using drug B offers increased opportunities for the emergence of double resistance, which is never the case with combination therapy.

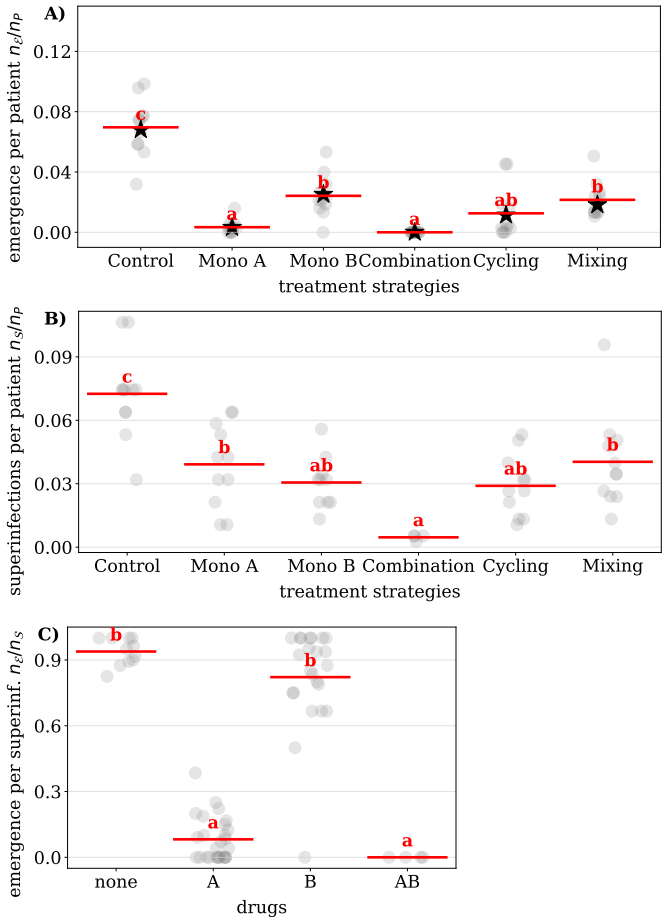

Fig. 2.3 Analysis of the emergence of double resistance in vitro and superinfection between single resistant A_r and B_r wells during the maximum-emergence scenario, from transfer four onwards. Each dot corresponds to data from a single plate, with each plate representing a distinct treatment arm, encompassing 376 patients for one transfer. Mean values are represented by red bars. Bars not sharing a letter are significantly different ($p < 0.05$, ANOVA tables and pairwise Tukey post hoc results can be found in Table S51 – S56). A) Number of newly emerged cases of double resistance per plate ($n_{\mathscr{E}}$), normalised to the total number of patients ($n_P = 376$). B) Number of superinfections per plate ($n_{\mathscr{S}}$), normalised to n_P. C) Proportion of superinfected wells treated with A, B, AB, or none that develop double resistance.

Computational model corroborates the robustness of experimental outcomes. The experiments are conducted by a liquid handling platform that carries out predefined instructions, specifying which infections occur and who is admitted or discharged. The instructions are randomized based on parameter sets we defined for each scenario, including the overall infection and turnover probability as well as the distribution of the resistance profiles of admitted patients. We call the entirety of all instructions that come up during one experiment an 'instruction set'. Due to the scale and technical complexity of the experiments, it was not feasible to carry out individual instruction sets for each replicate, so we opted to apply the same instruction sets for all replicates. This raises the question of whether the experimental results are a consequence of a specific instance of this random process and whether they are robust to the randomisation in the instruction set. To address this, we developed a discrete-time stochastic model comprising

94 individual in silico patients mimicking the epidemiological dynamics of the experiment (SI Computational Model). The model was parametrised, but not fitted, with transition probabilities (Table S18–S25) that we estimated based on the transition frequencies measured in vitro. We used the same transition probabilities in the simulations for all scenarios.

First, we validated the model by averaging 100 validation simulations, each employing the identical instruction sets used in vitro. The aim of the validation simulations is to recreate the experiments in silico (Figure S3B). We found that the simulation results are in good agreement with the experimental data, indicating that the model reflects the dynamics observed in the in vitro experiments well (see Fig. 2.2, Figure S2, and Figure S4). One exception is the spread of A-resistance during the prevention scenario in control and Mono A. This could indicate an increased number of contaminations at the beginning of the prevention scenario. We also observe some discrepancies for the spread of double resistance during the prevention scenario, which we attribute to contamination artefacts in the transition probabilities (see SI Computational Model).

Second, we averaged 100 variation simulations to assess the robustness of the experimental outcomes against variations in the instruction sets. In these variation simulations, each of the 100 instruction sets was randomized based on the same three parameter sets used in vitro (Figure S3C). Differences between the validation and variation simulations indicate differences in outcome due to the randomization of the instruction sets. For instance, with a turnover probability $\tau = 0.2$ and an admission probability $c_A = 0.05$, we expect 0.94 A_r admissions per transfer. However, random fluctuations can result in either more (or fewer) A_r admissions, leading to a temporarily higher (or lower) frequency of A_r in the validation simulations, creating a temporary spread between the validation and variation simulations. We observed that the validation simulations fluctuate around the variation simulations and never diverge far (see Fig. 2.2, Figure S2, and Figure S4), indicating robustness of the experimental results to the randomisation of the instruction sets.

***In silico* sensitivity analysis indicates that the superiority of combination therapy is robust.** Given that the validation simulations agreed well with the experiments, we used the model to perform an in silico parameter sensitivity analysis of the experimental results (Figure S3D). To this end, we ran ten simulations for each of 20,000 randomly generated parameter sets by varying the

turnover and infection probability and the five sampling proportions for incoming patients: (τ, β, c_S, c_{A_r}, c_{B_r}, c_{AB_r}, c_U). For half of the parameter sets, we forced the frequency of incoming patients with double resistance (c_{AB_r}) to zero.

We used the frequency of uninfected in silico patients to measure treatment success. Using this criterion, the control strategy (no treatment) always performed worst, and accordingly, we excluded this treatment arm from the following analysis. Strategies were then classified as (i) 'single winners' if they are significantly better than all other strategies; (ii) 'winners' if they are not outperformed by any other strategy; (iii) 'losers' if they do not outperform at least one other strategy; or (iv) 'single losers' if all other strategies outperform them.

In parameter sets with and without pre-existing double resistance, combination therapy ranks most often as one of the best strategies (87% and 98%, respectively). It is the single best strategy in 55% of the tested parameter sets with pre-existing double resistance and in 93% of cases without pre-existing double resistance (Fig. 2.4, Table S14, Table S15).

In some situations (for example, when one strategy is much worse than all others), it is more important to avoid the worst strategy than selecting the very best strategy among the good ones. Our analysis finds that combination therapy is almost never among the worst strategies, while usually one of the two monotherapies performs worst. As expected, single-drug strategies perform particularly poorly when there is a high frequency of pre-existing single-resistance to the applied drug (Table S11, Table S13).

Cycling and mixing lose substantially less than the monotherapies but are rarely the single best strategy.

2.4 Discussion

In our study, multi-drug strategies, particularly combination therapy, outperformed monotherapies in reducing overall infections and the emergence of double resistance across most scenarios, while we observed most emergence of double resistance in the untreated control. Interestingly, the effectiveness of combination therapy does not stem from an increased efficacy associated with higher doses. This is because an asymmetrical antagonism exists between the bactericidal antibiotic ceftazidime (drug A) and the bacteriostatic antibiotic tetracycline (drug B), resulting in a lower clearance rate for the combination A+B compared to drug A alone (SI Results). This

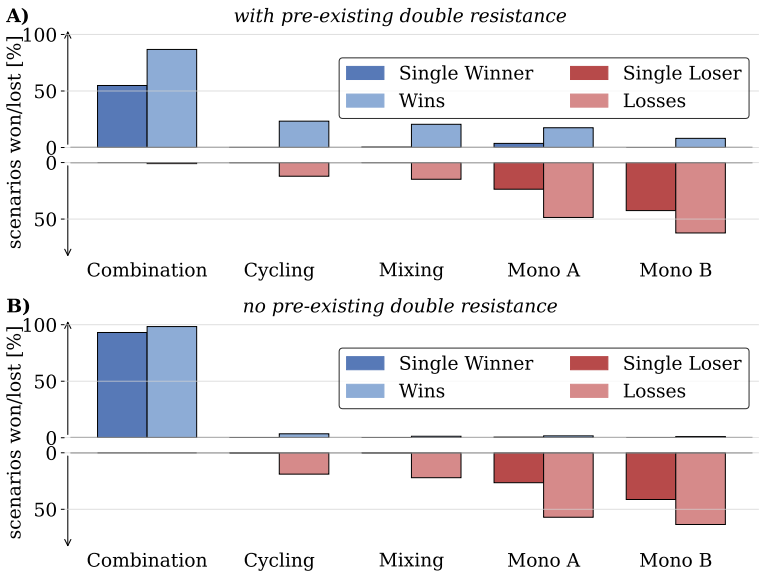

Fig. 2.4 Effectiveness of the five treatment strategies in maximising the frequency of uninfected individuals across randomly generated parameter sets. Strategies not significantly better than any other are marked as losers (pastel red), and those significantly worse than all others as single losers (dark red). Strategies not significantly worse than any other are classified as winners (pastel blue), and those significantly better than all others as single winners (dark blue). Strategies without significant differences were excluded. (A) 10,000 parameter sets with pre-existing double resistance. 606/10,000 sets yielded no significant difference between the strategies. (B) 10,000 parameter sets without pre-existing double resistance. 100/10,000 sets yielded no significant difference between the strategies.

observation implies that combination therapy may be even more advantageous when drugs are neutral or synergistic towards each other.

Why does the absence of treatment lead to worse outcomes, and why is combination therapy preventing the emergence of double resistance so effectively?

First, we measured the presence, not the density, of resistant bacteria in wells by assessing if small aliquots of the liquid culture could grow on treated agar plates. This approach quantifies the number of wells hosting a specific resistance but can not quantify the frequency of resistance in the in-well population. The information about presence/absence alone yields important information about potential treatment success and is used in analogous clinical diagnostic methods, such as disk diffusion tests European Committee on Antimicrobial Susceptibility Testing (EUCAST) (2024).

We would only recognize a loss of resistance (in the experiments and clinical samples) if the resistant strain were fully outcompeted. This was not observed during the containment scenario in the untreated control. Such an outcome was expected due to the short average patient stay of 2–5 days in our experiments and 5–6 days in clinical situations Hofstetter et al. (2017). For the same reason, we would not expect an eradication of resistance but only a shift in resistance density, even if there were more substantial costs of resistance or higher segregational loss. In our experiments, we found no evidence of a cost of resistance (see SI Methods, Figure S6, and Table S3) or segregational loss (see SI Methods and Table S4).

Second, in our experiments, the emergence of double resistance requires conjugation, which relies on superinfection between hosts with complementary resistance profiles. As demonstrated in Fig. 2.3B, the lowest number of superinfections occur in combination therapy, where both single-resistant strains can be cleared. Conversely, without treatment, the abundance of single resistance is highest resulting in the highest number of superinfections.

Third, the applied antibiotics affect the frequency of superinfections leading to double resistance, likely by influencing the growth dynamics within the superinfected well and potentially the conjugation rate Headd and Bradford (2018). However, our experimental data are unsuitable for supporting or rejecting the impact on conjugation rates. We observed the least emergence of double resistance in superinfected wells treated with both drugs and most in untreated wells, contributing to the superiority of combination therapy and the high rates of double resistance in the absence of treatment (Fig. 2.3C). This effect on the in-well dynamics may be a property of the chosen drugs and concentrations, and we expect better results for cycling and mixing if both drugs were equally effective in suppressing double resistance or worse results for combination therapy if the combination of both drugs was less effective.

Fourth, we observed that the number of single-resistant bacteria inoculating superinfections impacts the frequency of emerging double resistance (see SI Results, Table S1). In our setup, superinfected wells receive two inocula, with at least one inoculum transferred from the previous plate (by infection) that has already undergone treatment for one day. When prior treatment led to a low bacterial density in the source wells, we did not observe any cases of double resistance emerging. This could magnify the effectiveness of combination therapy, where all potential single-resistant inocula transferred from the previous plate contain low bacterial densities due

to effective treatment. On the one hand, this may be more a characteristic of our experimental setup due to the fixed length of the treatment interval and high clearance probabilities. On the other hand, we indeed expect fewer cases of emergence in superinfected patients if the infecting inocula are small.

In our experiments and simulations, combination therapy showed superior results in minimizing infections and preventing double resistance. This advantage may partly result from assumptions and simplifications, including the chosen strain, drugs, plasmids, and inoculum size, the discrete setup with fixed treatment durations, colonization-independent infection and turnover probabilities, and the absence of an immune system and microbiome. Also, treating all patients irrespective of colonization diverges from clinical reality in two ways: i) in a clinical setting, some untreated patients may serve as a sanctuary for resistance and a potential source of double resistance and ii) treating all patients, regardless of infection status, contrasts with clinical efforts to promote targeted antibiotic use. However, since patients as we model them in our in vitro experiments lack a microbiome, treating uninfecteds should have no impact on the resistance dynamics.

Despite the numerous differences between our experiments and a real clinical situation, we argue that the relative effectiveness of combination therapy in suppressing double resistance would likely translate to real patients. The reason is that the emergence of double resistance hinges on two critical processes: 1) preventing superinfections between patients carrying bacteria with complementary resistance plasmids and 2) the probability that superinfected hosts develop double resistance. We think that combination therapy offers a strategic advantage in addressing both processes.

Our results complement the findings by Angst et al. Angst et al. (2021), who observed similar outcomes in the context of chromosomal resistance. We believe that such in vitro experimental models, which explore admittedly idealised and simplified epidemiological scenarios, can help to bridge the divide between mathematical models and randomised clinical trials. However, ultimately the evidence for or against the benefits of combination therapy must be confirmed by rigorous clinical trials with sufficient statistical power to support or challenge the effectiveness of combination therapy.

2.5 Methods

Drugs and Media. In all experiments, we used LB (Sigma L3022) with 25 $\mu g/ml$ (prevention scenario) or 5 $\mu g/ml$ (containment and max-emergence scenario) chloramphenicol as a liquid medium and the same LB and drugs with 1.5% agar as a solid medium. Chloramphenicol was added to prevent external contaminations. We could not measure any significant growth effects of the chloramphenicol concentrations on the chloramphenicol-resistant strains (see Table S5). We used 80 $\mu g/ml$ ceftazidime as drug A and 40 $\mu g/ml$ tetracycline as drug B, with identical concentrations for liquid and solid media.

Strains and Plasmids. We used two compatible plasmids p_A and p_B derived from samples ESBL9 and ESBL25 from a clinical transmission study Tschudin-Sutter et al. (2016). Samples were kindly provided by Adrian Egli and sequenced and analysed by Huisman et al. Huisman et al. (2022). Plasmids p_A and p_B provide (among other resistances) resistance against drug A and drug B, respectively. We used these plasmids and the chloramphenicol-resistant host MDS42-YFP Fehér et al. (2012) (sensitive to drugs A and B) to create three additional strains by conjugation (Table S2) (i) A-resistant, containing p_A; (ii) B-resistant, containing p_B; and (iii) AB-resistant, containing both plasmids (see SI Methods).

Treatment arms. We simulated the epidemiological dynamics of six hospital wards in vitro, with each ward exploring a different treatment arm: (i) control with no treatment, (ii) monotherapy with ceftazidime (mono A), (iii) monotherapy with tetracycline (mono B), (iv) cycling therapy (A, A, B, B, ...), (v) mixing therapy (treatment A and B are randomly assigned daily, without knowledge of prior treatment), and (vi) combination therapy (treating all patients with both drugs, each at full concentration).

Assay plates. Each hospital ward was simulated in vitro on a 384-well microtiter plate (Greiner 781186). Wells are interpreted as beds in four replicate hospital wards with 94 beds each. The remaining wells contained only growth medium and remained untouched, acting as sentinels for contamination. Across all experiments and treatment arms, 2752 control wells were used, 67 of which became contaminated. Wells with growth medium but no bacteria represent uninfected patients, whereas wells with growth medium and (resistant or sensitive) bacteria represent infected patients.

Experimental procedure. Experiments were performed using a Tecan Evo 200 automated liquid handling system (Tecan) with an integrated, automated incubator (Liconic STX100, Liconic), a Tecan Infinite F200 spectrophotometer (Tecan), and a camera (Pickolo, SciRobotics).

Every day new assay plates were filled with 45 µl fresh medium and 5 µl antibiotic stock, according to its designated treatment strategy (see Figure S1). At each of these transfers, we simulate patients staying overnight in the hospital (passage), the admission and discharge of patients (turnover), and infections between patients (infection). Passage, turnover and infections were all done by inoculating the new plate using a pintool with retractable pins, as detailed below, carrying ≈0.3 µl drops between wells ($\approx 1:150$ dilution) leading to an approximately 6-8 hours exponential phase. The assay plates were then incubated at 37 °C and 95% relative humidity. The incubation duration varied due to variations in the time it takes to set up a new transfer and occasional transfer repetitions made necessary because of machine errors or user mistakes. The mean incubation duration was 27 hours.

We initiated the experiment by inoculating one 384-well plate from fresh overnight cultures representing patients from an outside community. We assume that this community is sufficiently large to be unaffected by interactions with the hospital ward. Incoming patients are either uninfected or carry one of the four strains (sensitive, each single resistant or double resistant) and are sampled according to predefined sampling proportions, defining the probability of a resistance profile being admitted to the hospital. (Table 2.1). This initial plate remained untreated and was used as the initial population for all six treatment arms.

Turnover. Every transfer, each patient has a turnover probability τ to be discharged from the hospital and replaced by a newly admitted patient. Wells representing staying patients were passed from the previous to the new assay plate using the pintool. Here, the pins for discharged patients are retracted. Vacant beds on the assay plate were then reoccupied by patients from the community analogous to the initial setup.

Infections. To simulate infections, each well has an infection probability β to infect another randomly chosen well on the next assay plate during the transfer. Therefore, each patient can infect at most one other patient per transfer, but several patients could potentially infect the same patient.

Resistance Profiles. To assess the resistance profile of each well, we spotted the previous assay plate onto four agar plates, using the pintool. Three plates were treated with antibiotics (A, B, or AB), while one was untreated (none). After incubation at 37 °C and 95% relative humidity, images of the agar plates are taken and analysed using the Pickolo package (SciRobotics, Kfar Saba, Israel). The software automatically detects the presence of colonies at each well position, which we also manually verified. The growth pattern on the four agar plates allowed us to determine the resistance profile of a well, which reflects how the well would behave if treated.

By default, we distinguish six resistance profiles (Table S6). The wells may either be 1) uninfected (U), 2) exclusively infected with sensitive bacteria (S), 3) infected with A-resistant bacteria (A_r), 4) infected with B-resistant bacteria (B_r), 5) infected with AB-resistant bacteria (AB_r), 6) or be infected with a mixed population containing A-resistant and B-resistant bacteria, but no AB-resistant bacteria ($(A\&B)_r$). The way we classify the resistance profiles of the bacterial population in a well leads to the dominance of resistance, in the sense that a predominantly sensitive population harbouring a resistant minority would be classified as resistant (see Table S7). Any observed growth pattern not corresponding to the six resistance profiles mentioned above is classified as 'other'. The resistance profile 'other' primarily occurs when bacterial densities are low (see also SI Methods).

Scenarios. We conducted experiments for three scenarios (prevention, containment, and maximum-emergence) with 14 to 27 transfers each. Each experiment was defined by a different parameter set consisting of (i) the infection probability β within the hospital, (ii) the turnover probability τ and (iii) the sampling proportions c_ϕ of patients with resistance profile $\phi \in \{U, S, A_r, B_r, AB_r\}$ (see Table 2.1).

The prevention scenario (Figure S2) addresses how the treatment strategies perform with a moderately resistant community and a moderate infection regime in the hospital ward and how well they are able to prevent the upcoming double resistance.

The containment scenario (Figure S4) corresponds to a scenario in which some patients entering the hospital are infected with double-resistant bacteria to compare the ability of treatment strategies to contain the spread of pre-existing double resistance.

During the maximum-emergence scenario (Fig. 2.2) 50 % of the incoming patients are infected

with A-resistant bacteria, and the other 50 % are infected with B-resistant bacteria. These conditions maximally favour opportunities for horizontal gene transfer. The basic reproduction number was set to $R_0 = 0.5$ (Equation S1) to ensure that double-resistant strains are flushed out, reducing the stochastic dependency on earlier emergence events while maintaining a high potential for new emergence.

Instruction Sets. Based on the parameter defined for each experiment (see Table 2.1), we generated instructions that were passed to the liquid handling platform. These instructions specify which patients are passaged or discharged and admitted, who infects whom, and the treatment for mixing therapy. Instructions are randomly generated prior to each transfer. We call the entirety of all instructions that come up during an experimental run an instruction set. Instruction sets are identical across all treatment arms and replicates.

Computational Model. We created a stochastic model (SI Computational Model) incorporating 94 in silico patients, each capable of adopting one of six resistance profiles $\phi \in \{U, S, A_r, B_r, AB_r, (A_r\&B_r)\}$. The model is structured analogue to the in vitro experiments (Figure S1) and alternates between modelling the transactions between wells and the effect of treatment during incubation.

Admission and discharge (turnover) were simulated by replacing the resistance profile of the current patient with that of the incoming patient, as defined by the instruction set. Infections are simulated by combining the resistance profiles of the receiving well i and the infecting well j. The resulting resistance profile $\phi_i + \phi_j$ is determined using the rules based on the dominance of resistance specified in Table S9. Calculations involving more than two resistance profiles apply the associative law and are determined pairwise, e.g. $(U + S) + A_r = S + A_r = A_r$.

To model treatment effects, we use transition probabilities to assign the post-incubation resistance profile $\phi(\hat{T})$ stochastically based on the treatment and the pre-incubation resistance profile $\phi(T)$. The transition probabilities (Table S18 – S25) were estimated based on experimental data across all experiments.

***In Silico* Sensitivity Analysis.** To augment the experimental data, we conducted an in silico sensitivity analysis. We randomly generated 10,000 parameter sets with and 10,000 without pre-existing double resistance. Turnover and infection probabilities were uniformly sampled

$[0.05, 0.95]$, allowing for $R_0 \in [0.0526, 19]$. The sampling proportions c_ϕ for all incoming resistance profiles ($\phi \in \{U, S, A_r, B_r, AB_r\}$) were randomised by sampling a number $n_\phi \in [0, 1]$ from a uniform distribution and subsequently normalising by the sum: $c_\phi = n_\phi / \sum_j n_j$. We created ten randomised instruction sets for each parameter set and conducted one simulation per instruction set (Figure S3D) for 28 transfers.

For this analysis, the frequency of non-infected individuals during the last four transfers was used as a performance metric for treatment strategies, as it also indirectly reflects the frequency of both double- and single-resistant patients. We conducted an ANOVA test to assess if the effect of the treatment strategies significantly ($p < 0.05$) influences the frequency of uninfecteds. For significant tests, we proceeded with Tukey's post hoc analysis ($p < 0.05$), identifying significantly distinct pairs of strategies. Strategies not significantly inferior to others were classified as 'winners', while strategies not significantly superior to any were classified as 'losers'. Strategies that win or lose a parameter set alone are 'single winners' or 'single losers'.

Data Availability Experimental data and analysis scripts, as well as code for the computational model, have been deposited in Zenodo (`https://doi.org/10.5281/zenodo.14137410`).

Acknowledgments

We thank Adrian Egli for generously providing the ESBL samples containing the plasmids and Fabienne Benz and Jana Huisman for their assistance with selecting them. We also thank Lukas Graz from the Seminar for Statistics (ETHZ) for his statistical consultation. We used Grammarly and OpenAI's ChatGPT for proofreading and grammar checking. We thank ETH Zurich for providing funding.

BIBLIOGRAPHY

P. F. Kable and H. Jeffery. Selection for Tolerance in Organisms Exposed to Sprays of Biocide Mixtures: A Theoretical Model. Phytopathology, 70(1):8–12, 1980. ISSN 0031-949X. doi: 10.1094/phyto-70-8.

Charles J. Delp. Coping with resistance to plant disease. Plant Dis., 64:652–657, 1980. doi: 10.1094/PD-64-652.

George Skylakakis. Effects of Alternating and Mixing Pesticides on the Buildup of Fungal Resistance. Phytopathology, 71(11):1119 – 1121, 1981. ISSN 0031-949X. doi: 10.1094/phyto-71-1119.

Daniel E. Goldberg, Robert F. Siliciano, and William R. Jacobs. Outwitting evolution: Fighting drug-resistant TB, Malaria, and HIV. Cell, 148(6):1271–1283, 2012. ISSN 10974172. doi: 10.1016/j.cell.2012.02.021.

Berit Siedentop, Viacheslav N Kachalov, Christopher Witzany, Matthias Egger, D Roger, and Sebastian Bonhoeffer. The effect of combining antibiotics on resistance : A systematic review and meta-analysis. Elife, 13:1–25, 2024. doi: 10.7554/eLife.93740.1.

Pleun Joppe van Duijn, Walter Verbrugghe, Philippe Germaine Jorens, Fabian Spöhr, Dirk Schedler, Maria Deja, Andreas Rothbart, Djillali Annane, Christine Lawrence, Jean Claude Nguyen Van, Benoit Misset, Matjaz Jereb, Katja Seme, Franc Šifrer, Viktorija Tomiç, Francisco Estevez, Jandira Carneiro, Stephan Harbarth, Marinus Johannes Cornelis Eijkemans, Marc Bonten, Herman Goossens, Surbhi Malhotra-Kumar, Christine Lammens, Jordi Vila, and Ignaci Roca. The effects of antibiotic cycling and mixing on antibiotic resistance in intensive care units: a cluster-randomised crossover trial. Lancet Infect. Dis., 18(4):401–409, 2018. ISSN 14744457. doi: 10.1016/S1473-3099(18)30056-2.

Hildegard Uecker and Sebastian Bonhoeffer. Antibiotic treatment protocols revisited: The challenges of a conclusive assessment by mathematical modelling. J. R. Soc. Interface, 18(181), 2021. ISSN 17425662. doi: 10.1098/rsif.2021.0308.

Sebastian Bonhoeffer, Marc Lipsitch, and Bruce R. Levin. Evaluating treatment protocols to prevent antibiotic resistance. Proc. Natl. Acad. Sci. U. S. A., 94(22):12106–12111, 1997. ISSN 00278424. doi: 10.1073/pnas.94.22.12106.

Burcu Tepekule, Hildegard Uecker, Isabel Derungs, Antoine Frenoy, and Sebastian Bonhoeffer. Modeling antibiotic treatment in hospitals: A systematic approach shows benefits of combination therapy over cycling, mixing, and mono-drug therapies. PLoS Comput. Biol., 13(9):1–22, 2017. ISSN 15537358. doi: 10.1371/journal.pcbi.1005745.

Daniel C. Angst, Burcu Tepekule, Lei Sun, Balázs Bogos, and Sebastian Bonhoeffer. Comparing treatment strategies to reduce antibiotic resistance in an in vitro epidemiological setting. Proc. Natl. Acad. Sci. U. S. A., 118(13):1–7, 2021. ISSN 10916490. doi: 10.1073/PNAS.2023467118.

Jana S. Huisman, Timothy G. Vaughan, Adrian Egli, Sarah Tschudin-Sutter, Tanja Stadler, and Sebastian Bonhoeffer. The effect of sequencing and assembly on the inference of horizontal gene transfer on chromosomal and plasmid phylogenies. Philos. Trans. R. Soc. B Biol. Sci., 377(1861), 2022. ISSN 14712970. doi: 10.1098/rstb.2021.0245.

Sarah Tschudin-Sutter, Reno Frei, Friedbert Schwahn, Milanka Tomic, Martin Conzelmann, Anne Stranden, and Andreas F. Widmer. Prospective validation of cessation of contact precautions for extended-spectrum β-lactamase-producing Escherichia coli1. Emerg. Infect. Dis., 22(6):1094–1097, 2016. ISSN 10806059. doi: 10.3201/eid2206.150554.

European Committee on Antimicrobial Susceptibility Testing (EUCAST). Antimicrobial susceptibility testing EUCAST disk diffusion method Version 12.0 January, 2024.

Kathrin Hofstetter, Edith Salgado-Thalmann, and Marc Bachmann. Kennzahlen der Schweizer Spitäler 2015, 2017.

Brendan Headd and Scott A. Bradford. Physicochemical factors that favor conjugation of an antibiotic resistant plasmid in non-growing bacterial cultures in the absence and presence of antibiotics. Front. Microbiol., 9:1–14, 2018. ISSN 1664302X. doi: 10.3389/fmicb.2018.02122.

Tamás Fehér, Balázs Bogos, Orsolya Méhi, Gergely Fekete, Bálint Csörg, Károly Kovács, György Pósfai, Balázs Papp, Laurence D. Hurst, and Csaba Pál. Competition between transposable elements and mutator genes in bacteria. Mol. Biol. Evol., 29:3153–3159, 2012. ISSN 0737-4038. doi: 10.1093/molbev/mss122.

3 MSB paper

Some text here

4 Combination Paper

some text here

5 Concluding Remarks

some text here